Materials Science-Poland
Volume 42 Issue 4 · pp. 11–20 · DOI: 10.2478/msp-2024-0041

Materials Science-Poland

Synthesis, characterization, and applications of a novel poly(4-[pyrrol-1-yl methyl]benzoic acid)–silver composite

Research Article

M. I. Benamrani*, I. Chikouche, A. Zouaoui

Laboratoire: Croissance et Caractérisation de Nouveaux Semiconducteurs (LCCNS), Faculté de Technologie, Université Ferhat Abbas Sétif 1, 19000, Sétif, Algeria

Received 12 July 2024; Accepted 02 September 2024

Abstract: This article describes the manner in which a novel composite compound was synthesized using a novel method and optimized using a poly(4-[pyrrol-1-yl methyl]benzoic acid) (PPy-b) polymer and very little amount of metallic silver microparticles. The deposition of the polymer film on a fluorine-doped tin oxide (FTO) substrate surface was performed by electrochemical oxidation of the monomer in acetonitrile medium at an imposed potential. The incorporation of silver microparticles was carried out by immersing the modified electrode in a solution of silver nitrate to complex the Ag^+ ions with the carboxylic group (COOH) present in the backbone of the polymer, followed by an electrochemical reduction of the complex to precipitate the silver in the form of metallic microparticles in the polymer film. Different characterization techniques (cyclic voltammetry, electrochemical impedance spectroscopy, and surface analysis techniques) were used to optimize the prepared material. Despite the very small quantity of silver (a few micrograms), inserted into the polymer film, the composite material thus obtained had good electrical, optical, and catalytic properties.

Keywords: *Conductive polymer • Polypyrrole • Composites • Silver microparticles • Catalysis • Diodes*

1. Introduction

Composite materials of the (polymer–metal) type prepared from films of conductive polymers, such as polypyrrole, polyaniline, and polythiophene [1–5], and metallic particles of noble metals, transition metals, and metal oxides are of considerable interest in various fields such as catalysis, analysis, energy storage, electrochemical sensors, optoelectronics, and electronics.

The deposition of a polymer thin film on an electrode surface by electropolymerization of a monomer is currently one of the highly developed methods. It consists of polymerizing a monomer either by oxidation or by electrochemical reduction, and the insoluble polymer thus formed is deposited on the electrode surface in the form of multilayers. Herein, it is worth noting that the main advantage of the electrochemical method is the direct control of the amount of polymer deposited by coulometry, also leading to the control of the thickness of the deposited film. At this level, it seems useful to us to point out that the polymer films obtained are stable, uniform, strongly adherent, and insoluble in organic solvents.

The synthesis of composite materials by depositing a film of polypyrrole and silver particles on different supports according to different methods, namely chemical, electrochemical, microemulsion, or photopolymerization, has led to effective electrode materials for the detection of glucose [6], oxygen peroxide [7,8], ammonia [9,10], nitrates [11], and hydrazine [12], in corrosion protection [13], and in supercapacitors [14–16]. These modified electrodes also exhibit considerable antibacterial activity [17].

The objective of our study is to present a novel method for the synthesis of a new composite compound based on poly(4-[pyrrol-1-yl methyl]benzoic acid) (PPy-b) and silver. Characterization of the material was carried out through

* *E-mail: marouaimene.benamrani@univ-setif.dz*

the use of different analysis techniques (electrochemical, spectroscopic, electrical, and surface analysis). Finally, some potential applications of the new composite material such as in catalysis and electronics are presented.

2. Materials and methods

2.1 Electrochemical instrumentation and reagents

All the electrochemical experiments were carried out using a Biologic SP300 potentiostat controlled by a computer through the use of EC-Lab software. A conventional Metrohm cell with a volume of 10 ml consisting of three electrodes was used. The working electrode was a fluorine-doped tin oxide-coated glass (FTO/glass) slide substrate obtained from Sigma Aldrich with a surface area of 0.25 cm^2 and having a surface resistivity of ~7 Ω/sq, the auxiliary electrode was a carbon rod and the reference electrode was a saturated calomel electrode (SCE). The monomer (pyrrol-1-yl methyl)benzoic acid was synthesized according to the procedure described by Deronzier and Marques [18]. Silver nitrate, lithium perchlorate, sodium nitrate, and acetonitrile were all commercial products.

2.2 Electrochemical impedance spectroscopy (EIS)

EIS was used to investigate the properties of the composite material. It is a well-documented material analysis tool [19]. The measuring frequency range was from 100 kHz to 10 mHz with the signal amplitude set to 10 mV. The resulting Nyquist curves were recorded at an open-circuit potential. The charge transfer resistance value was extracted from the interception of the complex impedance diagram with the real-axis.

2.3 Four-point probe resistivity method

The equipment from Signatone (PRO4) was commonly used to measure the surface resistivity value of a layer of materials and in characterizing the electrical conductivity of thin films. It was managed by a software that controls a Keithley 2450 source. The latter provides a current fed through the outer two probes and measures the voltage across the inner two probes. The software determines the sheet resistivity value for a given sample thickness. The same equipment was also used to measure the $I(V)$ characteristics of the devices.

2.4 Other measuring techniques

The samples' thicknesses were determined using a mechanical profilometer, Alpha-Step D-500 stylus profiler from KLA-Tencor. It is a microscope type that gives information on the topography and determines with a high precision the thickness of thin film materials.

In addition, the following characterization tools were used: a scanning electron microscope – JCM-5000 from JEOL, an X-ray fluorescence (XRF) spectrometer – Rigaku ZSX Primus IV, and an atomic force microscope – MFD-3D from Asylum Research.

3. Results and discussion

3.1 Electrochemical analysis

3.1.1 Electrochemical behavior of silver

The electrochemical behavior of silver was studied by cyclic voltammetry on an FTO/glass electrode in an aqueous solution containing 0.1 M $NaNO_3$ and 5×10^{-2} M silver nitrate ($AgNO_3$). The first cycle is shown in Figure 1a. The obtained curve is characterized by the presence of a reduction peak in the vicinity of a 0.28 V/SCE corresponding to the reduction of silver cations (Ag^+) to metallic silver (Ag). In the reverse scan, an intense oxidation peak is observed in the vicinity of a 0.53 V/SCE corresponding to silver oxidation of the deposited Ag^+.

Successive scans in the same domain (Figure 1b) show a very slight increase in redox peaks. This result is due to the modification of the surface state of the FTO/glass electrode during the scans.

Investigations were carried out in order to optimize the parameters of silver deposition on the FTO/glass substrate. They include the concentration of the silver solution, the scanning speed, the charge passed by imposing a potential on the electrodes, and the pH of the electrolyte solution. The latter was adjusted by adding a few drops of HNO_3. It was noticed that a significant displacement of the silver oxidation peak reduced during the reduction toward the less positive potentials by increasing the acidity of the medium and a clear increase in the intensity of the current peaks of reduction and oxidation. Indeed, silver reduces better at more acidic pH.

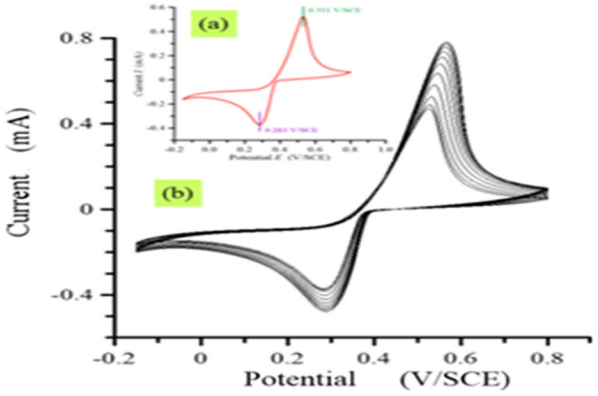

Figure 1. Voltammograms of silver recorded from an FTO/glass electrode immersed in an aqueous solution containing 0.1 M $NaNO_3$ and 5×10^{-2} M $AgNO_3$ at υ = 100 mV/s with pH 5. (a) First run and (b) successive scans.

3.1.2 Electrochemical behavior of the monomer

The cyclic voltammetry method was used to investigate the electrochemical behavior of the monomer 4-[pyrrol-1-yl methyl]benzoic acid on an FTO/glass electrode. The electrolyte solution contained 4×10^{-3} M monomer, 10^{-1} M acetonitrile (CH_3CN), and 10^{-1} M lithium perchlorate ($LiClO_4$). The cyclic voltammetry curve presented in Figure 2a is characterized by the presence of an irreversible oxidation peak around 1.3 V/SCE corresponding to monomer oxidation and consequently to the formation of a polymer film PPy-b deposited on the electrode surface (FTO/glass).

Successive scans between 0 and 1.4 V/SCE led to the appearance of a redox system (E_{Ox} = 0.9 V/SCE and E_{Red} = 0.5 V/SCE), which corresponds to the reversible oxidation of the polymer, Figure 2b. The progressive increase in the oxidation and reduction peaks is explained by the growth of a polypyrrole film deposited on the surface of the electrode.

3.1.3 Insertion of silver into the polymer film

In order to insert the silver in metallic microparticles form into the polymer film, the electrode polymer/FTO/glass, which was modified by the film of PPy-b, has been dipped in a solution containing 10^{-1} M silver nitrate ($AgNO_3$) during 30 min to complex the silver cations (Ag^+) with the polymer, then rinsed with distilled water to remove the excessive Ag^+ not retained by the polymer film. The modified electrode was then reduced to 0.35 V/SCE in an aqueous solution of 10^{-1} M sodium nitrate ($NaNO_3$) in the absence of silver to precipitate the complexed silver in the form of metal microparticles.

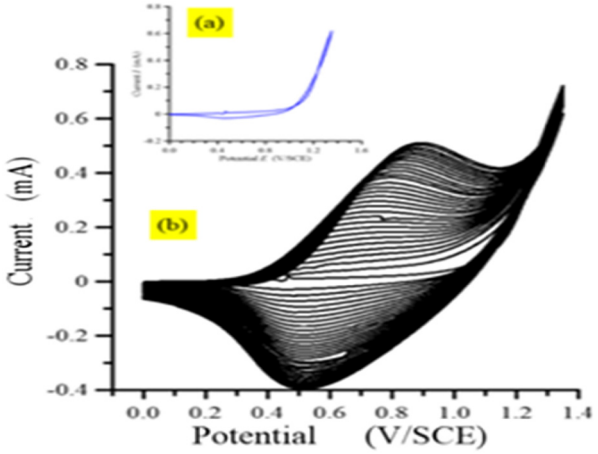

Figure 2. Cyclic voltammetry curves of the monomer on an FTO/glass electrode recorded from a solution containing 4×10^{-3} M monomer, 10^{-1} M acetonitrile, and 10^{-1} M $LiClO_4$, at the scanning speed of υ = 100 mV/s. (a) First run and (b) successive scans.

To ascertain that silver has been inserted into the polymer film, an oxidation of the modified electrode was carried out by scanning in the silver oxidation zone. The first run of the cyclic voltammetry recorded curve, Figure 3a, is characterized by an oxidation peak in the vicinity of 0.46 V/SCE attributed to the dissolution of the silver inserted into the polymer film. In the reverse scan, a reduction peak around 0.3 V/SCE was observed, which is attributed to the reduction of silver ions formed during the dissolution of the silver.

This result unambiguously confirms the insertion of metallic silver particles in the PPy-b film. The successive scanning, depicted in Figure 3b, showed a stability of the intensity of the oxidation and reduction peaks of silver. It seems that the silver particles are retained by the polymer film during their dissolution in Ag^+.

3.2 Characterization

3.2.1 EIS analysis

EIS of the elaborated thin films prior to and after insertion of silver particles into the polymer was carried out at an open circuit potential in the frequency range of 100 kHz to 10 mHz. Nyquist diagrams obtained are shown in Figure 4. A zoom-in view in the region of low impedance is shown in Figure 4b. The shape of the diagram corresponding to the FTO electrode (curve A) is almost a straight line, characteristic of the diffusion process of a semiconductor-type material. This was recorded at an open-circuit voltage of −0.0325 V. Meanwhile, the diagram plot recorded at an open-circuit voltage of 0.025 V of the deposited polymer film PPy-b exhibited a semicircular arc in the region of high frequency (curve B) due to charge transfer processes. After complexation of the Ag^+ cations with the polymer film and the reduction of the complex of polymer and silver in metallic microparticles (curve C), a clear reduction in the charge transfer resistance is observed, confirming the modification of the electrode surface and the insertion of the metallic silver microparticles. Herein, the diagram was recorded at an open-circuit voltage of 0.104 V. It exhibits a semicircular arc in the region of high frequencies attributed to charge transfer processes, followed by a straight line due to diffusion processes.

The electrical equivalent circuits that fit the Nyquist diagrams of curves B and C are depicted in Figure 4(b). Herein, R_s is the solution resistance, R_{ct} is the charge transfer resistance, C_p is the parallel capacitor, and Z_W is the Warburg impedance. Table 1 presents the fitted values of the electrical equivalent circuits of the electrochemical impedance measurements of curves B and C. It is worth noting the improvement in the electrical properties following the introduction of silver into the polymer film. For instance, the charge transfer resistance is reduced by 17 times once silver has been inserted and reduced.

It is worth noting that different species produces different behavior in EIS data. For instance, the insertion of silver shows a different behavior in comparison to that of cobalt [20].

3.2.2 Four-point probe sheet resistivity

Resistivity is the function of film thickness, which was determined using the mechanical profilometer. Table 2

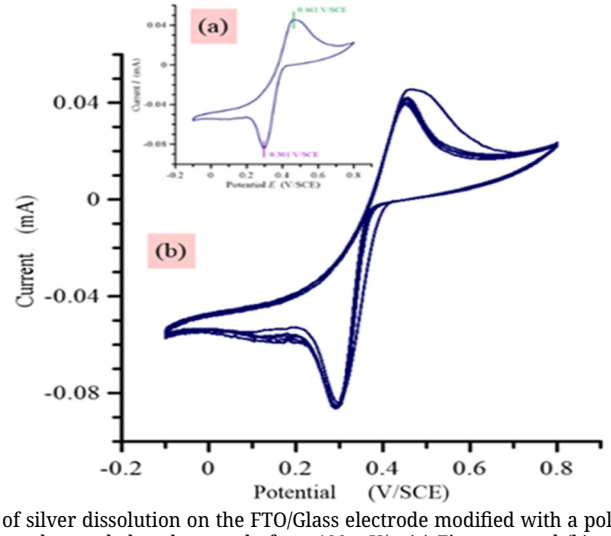

Figure 3. Cyclic voltammograms of silver dissolution on the FTO/Glass electrode modified with a polymer film in an aqueous solution containing 0.1 M $NaNO_3$ and recorded at the speed of υ = 100 mV/s. (a) First run and (b) successive scans.

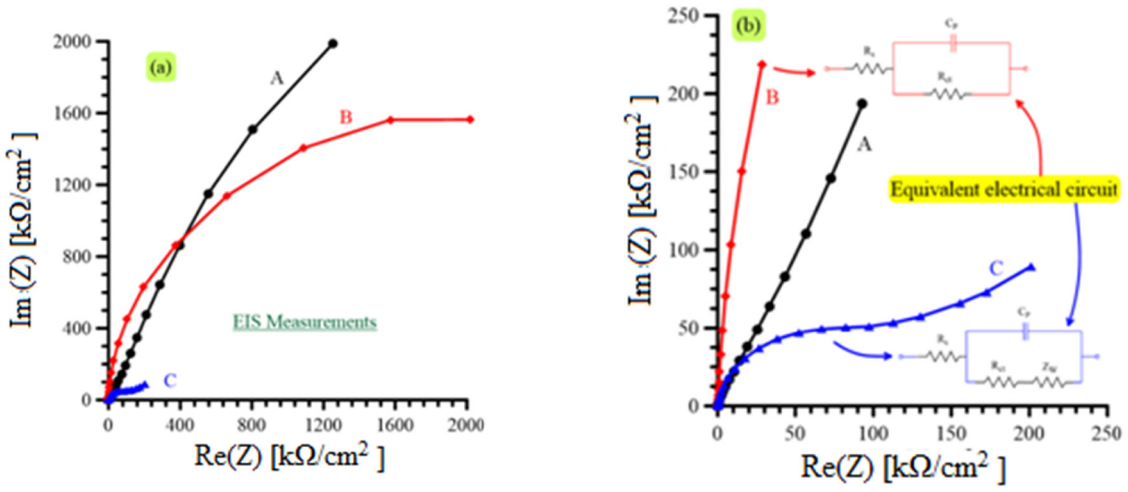

Figure 4. (a) Nyquist diagrams of the FTO electrode prior to and after insertion of silver microparticles into the polymer film PPy-b relative to: (A) FTO electrode, (B) FTO electrode modified by the polymer film, and (C) after insertion and reduction of silver microparticles into PPy-b. (b) A zoom-in view of the region of low impedance.

Electrode	R_s (Ω)	R_{ct} (MΩ)	C_p (μF)	Z_W (kΩ/s^{½})
PPy-b/FTO	164	2.87	2.93	—
Ag + PPy-b/FTO	107	0.164	4.28	98.9

Table 1. Fitted values of the components of electrical equivalent circuits of EIS data.

presents the average measured resistivity values (ten spots at different positions on the surface of each sample) of different specimens. Here again, the decrease in the specimen resistivities confirms the insertion of silver into the backbone of the polymer, and thus improves the conductivity.

3.2.3 Scanning electron microscopy (SEM) characterization

Figure 5 shows the SEM images of a film of the polymer PPy-b of 385 nm thickness (1.5×10^{-7} moles) deposited on an FTO substrate (Figure 5a) and that of the composite material (polymer–silver) (Figure 5b). Examination of the surface of the polymer shows that it has a more or less uniform globular morphology. After insertion of silver (1.2×10^{-7} moles ~ equivalent to 10^{-5} g) into the polymer film by immersion of an FTO electrode modified by the polymer film, a more concentrated globular morphology with varying grain sizes is observed on the entire surface. The bright spots observed indicate the presence of silver microparticles. This was confirmed by XRF analysis shown in Figure 6. The spectrum looks similar to that recorded using energy-dispersive spectroscopy (EDS) [17].

Film	FTO	PPy-b	PPy-b + Ag
Thickness (nm)	550	385	385
Resistivity (Ω cm)	8.22×10^{-4}	12.2×10^{-4}	7.4×10^{-5}

Table 2. Measured thickness and resistivity data.

3.2.4 Atomic force microscopy (AFM) characterization

The AFM image, illustrated in Figure 7a, taken from a part of the polymer film deposited on an FTO/glass substrate is observed to adopt a pyramidal shape with a square and a triangular base with a height of 1.25 μm and a roughness of 157.028 nm. After the insertion of silver microparticles into the polymer film by immersing the electrode in a solution of silver nitrate for 30 min and electrochemical reduction at 0.35 V, a clear modification of the surface of the material is observed, Figure 7b, due to the covering of the pyramids with silver particles. This is confirmed by the increase in the height of the substrate from 1.25 to 2 μm. Its roughness is on the order of 349.462 nm.

3.2.5 Optical properties

These were investigated using a spectrophotometer in the wavelength range 300–1,100 nm. The transmission spectra of different samples are shown in Figure 8.

The spectrum recorded of the substrate (FTO/glass) (curve A), whose *y*-axis is on the right, shows at the start, λ = 300 nm, an almost zero transmission rate to reach 90%

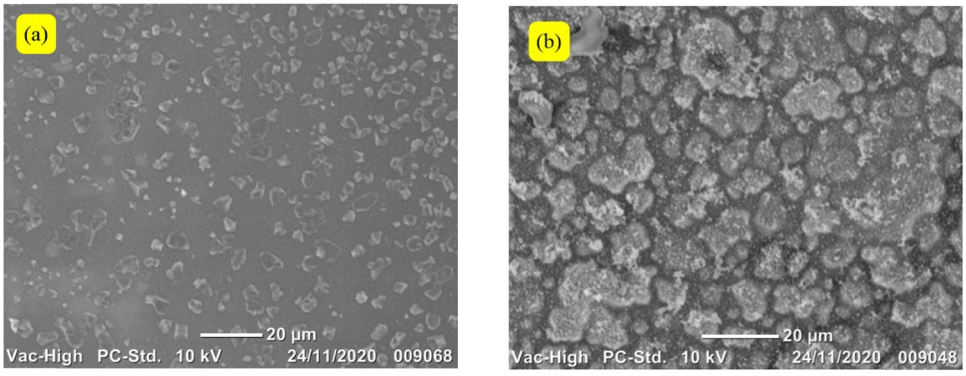

Figure 5. SEM surface images of: (a) a film of PPy-b deposited on an FTO electrode and (b) a modified FTO/polymer (PPy-b) electrode after insertion and reduction of silver microparticles.

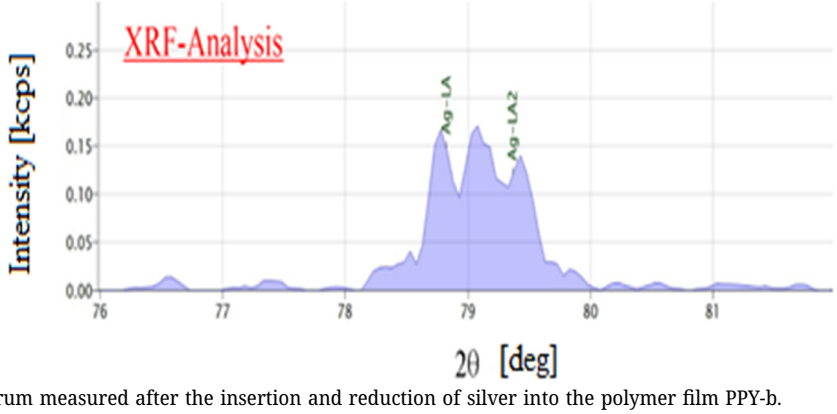

Figure 6. XRF spectrum measured after the insertion and reduction of silver into the polymer film PPY-b.

from λ = 330 nm and remains constant throughout the studied range. The starting spectrum behavior is due to the bandgap of FTO [21]. The transmission spectrum of the substrate modified by the polymer of thickness 385 nm is completely different (curve B), with its *y*-axis being always on the right. It displays a transmission rate of around 50% in the wavelength range λ = 700–950 nm. After the insertion of silver particles, the recorded spectrum (curve C), whose *y*-axis is on the left, displays new energy absorption bands, the first at λ = 500 nm and the second at λ = 700 nm. A clear reduction in the rate of transmission is observed (from 40 to 0.7%).

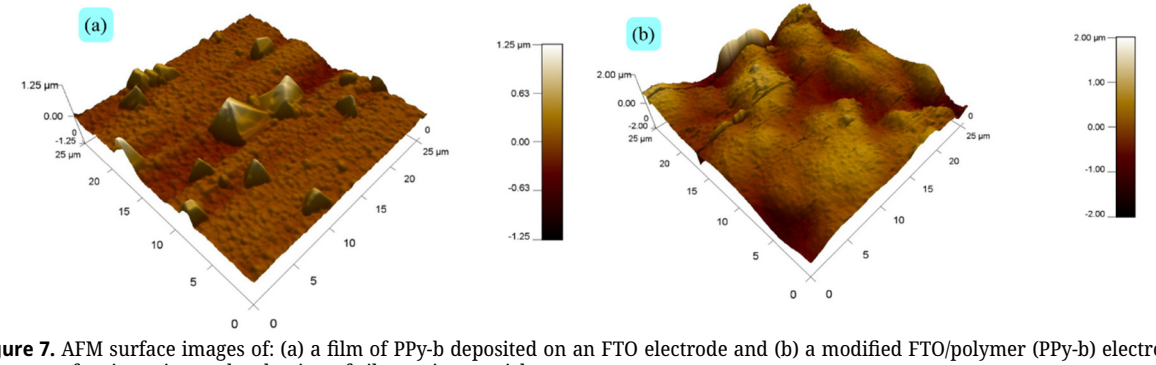

Figure 7. AFM surface images of: (a) a film of PPy-b deposited on an FTO electrode and (b) a modified FTO/polymer (PPy-b) electrode after insertion and reduction of silver microparticles.

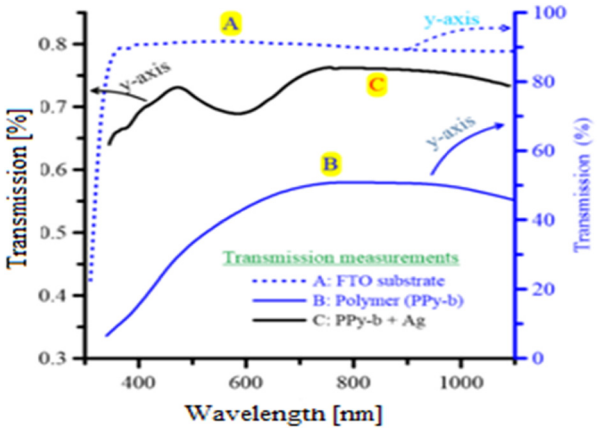

Figure 8. Spectral distributions recorded from the films in the UV–visible range. Curve A: FTO substrate; curve B: polymer; curve C: inserted silver.

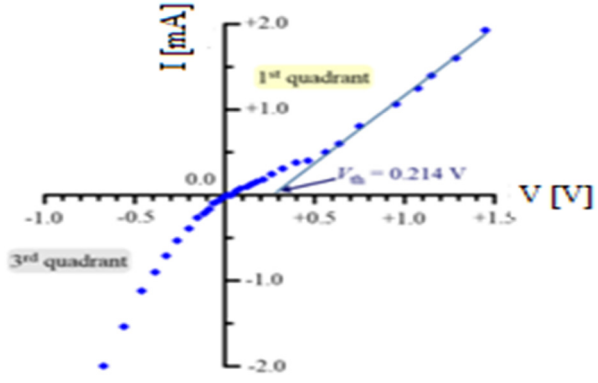

Figure 9. Characteristic *I*(*V*) of the composite (polymer + Ag)/FTO.

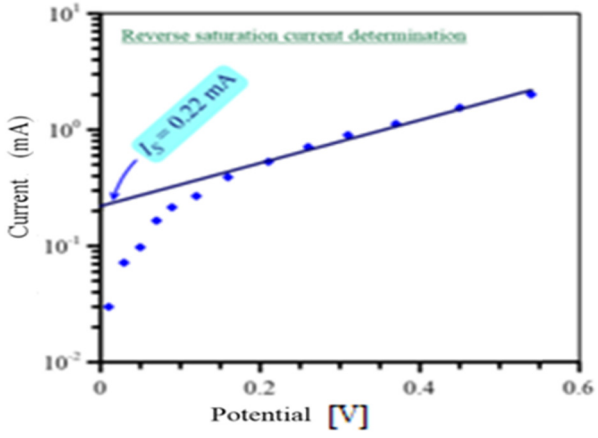

Figure 10. Determination of the reverse saturation current of the composite.

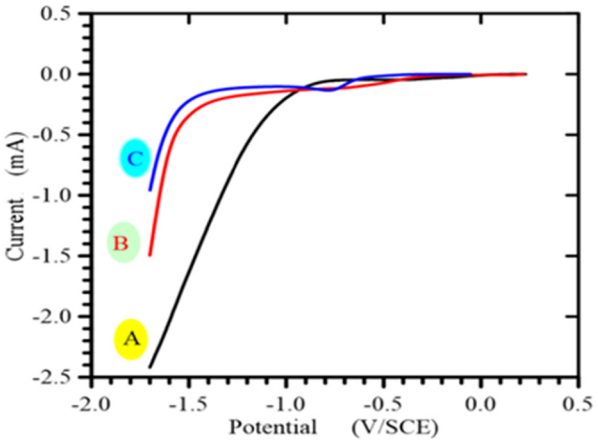

Figure 11. Recorded voltammograms of water reduction in 0.1 M NaOH of different electrodes at the scanning speed of 100 mV/s.

3.3 Applications

3.3.1 Electronic diodes

The $I(V)$ characteristic of the device based on the composite (polymer–Ag) as deposited on the FTO substrate was measured. It should be mentioned that there was no deposition of electrical contacts and that the measurements were carried out directly of the sample, whether on the substrate or on the polymer sides. The shape of the curve obtained, shown in Figure 9, corresponds to that of a diode. The value of the threshold voltage which is determined by extrapolation of the linear part (first quadrant of the characteristic) is V_{th} = 0.214 V.

The reverse saturation current of such configuration was also determined by using the characteristic $I(V)$ in a semilogarithmic scale (third quadrant). This is shown in Figure 10. Extrapolation of the linear part to V = 0 yields a reverse saturation current I_s = 0.22 mA. These parameters (V_{th} and I_s) are very appropriate for low power electronics applications [22–24].

3.3.2 Catalysis

Another potential application of the new composite material that has been investigated was in water reduction. The electrocatalytic effect of the composite material was tested in 0.1 M NaOH medium according to the following reaction:

$$2H_2O + 2e^- \rightarrow H_2 + 2OH^-. \quad (1)$$

The voltammograms obtained, shown in Figure 11, show a displacement of the hydrogen release overvoltage after the insertion of the metallic silver particles in the polymer film (curve C) as compared to that of the substrate (curve A) and after modification by the polymer film (curve B). This result clearly shows the good electrocatalytic activity of the composite material. Indeed, a potential gain estimated at 350 mV has been obtained.

4. Conclusions

This study present the synthesis and characterization results of a new composite material based on a polymer film PPy-b containing silver microparticles. This material was then investigated in the fields of electronics, optics, and catalysis. Electrochemical studies have shown the insertion of silver particles into the polymer film by complexation of Ag^+ ions in the polymer film, followed by its electroreduction to precipitate silver in the form of metallic microparticles. Electrochemical, spectroscopic (EIS and UV–visible), and morphological (SEM and AFM) characterizations confirmed the insertion of dispersed silver in the polymer film. This new composite material has good electrical (very low electrical conductivity), optical (a direct band gap E_g = 1.76 eV, suitable for photovoltaic cells), and catalytic properties (water reduction) despite the very small amount of silver being used.

Acknowledgements

The authors acknowledge the support from the Directorate General for Scientific Research and Technological Development (DGRSDT-Algeria).

Funding information

Authors state no funding involved.

Author contributions

Conceptualization: M.I. Benamrani; Formal analysis: M.I. Benamrani; Methodology: M.I. Benamrani, A. Zouaoui, I. Chikouche; Validation: M.I. Benamrani.

Conflict of interest statement

Authors state no conflict of interest.

References

[1] Pang, A.L., Arsad, A., Ahmadipour, M., Synthesis and factor affecting on the conductivity of polypyrrole: A short review, Polym. Adv. Technol., 2021, 32: 1428. doi: 10.1002/pat.5201

[2] Gor'kov, K.V., Talagaeva, N.V., Kleinikova, S.A., Dremova, N.N., Vorotyntsev, M.A., Zolotukhina, E.V., Palladium-polypyrrole composites as prospective catalysts for formaldehyde electrooxidation in alkaline solutions, Electrochim. Acta, 2020, 345: 136164. doi: 10.1016/j.electacta.2020.136164

[3] Babel, V., Hiran, B.L., A review on polyaniline composites: Synthesis, characterization, and applications, Polym. Compos., 2021, 42: 3142. doi: 10.1002/pc.26048

[4] Inagaki, C.S., Oliveira, M.M., Bergamini, M.F., Marcolino-Junior, L.H., Zarbin, A.J.G., Facile synthesis and dopamine sensing application of three component nanocomposite thin films based on polythiophene, gold nanoparticles and carbon nanotubes, J. Electroanal. Chem., 2019, 840: 208. doi: 10.1016/j.jelechem.2019.03.066

[5] Kaloni, T.P., Giesbrecht, P.K., Schreckenbach, G., Freund, M.S., Polythiophene: From fundamental perspectives to applications, Chem. Mater., 2017, 29: 10248. doi: 10.1021/acs.chemmater.7b03035

[6] Poletti Papi, M.A., Caetano, F.R., Bergamini, M.F., Marcolino-Junior, L.H., Facile synthesis of a silver nanoparticles/polypyrrole nanocomposite for non-enzymatic glucose determination, Mater. Sci. Eng. C Mater Biol. Appl., 2017, 75: 88. doi: 10.1016/j.msec.2017.02.026PMID: 28415543

[7] Mahmoudian, M.R., Alias, Y., Basirun, W.J., Woi, P.M., Yousefid, R., Synthesis of polypyrrole coated silver nanostrip bundles and their application for detection of hydrogen peroxide, J. Electrochem. Soc., 2014, 161: H487. doi: 10.1149/2.0571409jes

[8] Hnida, K.E., Socha, R.P., Sulka, G.D., Polypyrrole–silver composite nanowire arrays by cathodic co-deposition and their electrochemical properties, J. Phys. Chem., 2013, C117: 19382. doi: 10.1021/JP4038304

[9] Kiani, G., Nourizad, A., Nosrati, R., In-situ chemical synthesis of polypyrrole/silver nanocomposite for the use as a room temperature ammonia gas sensor, Fibers Polym., 2018, 19: 2188. doi: 10.1007/s12221-018-8097-z

[10] Yang, X., Li, L., Yan, F., Polypyrrole/silver composite nanotubes for gas sensors, Sens. Actuators B Chem., 2010, 145: 495. doi: 10.1016/j.snb.2009.12.065

[11] Bonyani, M., Mirzaei, A., Leonardi, S.G., Neri, G., Silver nanoparticles/polymethacrylic acid (AgNPs/PMA) hybrid nanocomposites-modified electrodes for the electrochemical detection of nitrate ions, Measurement, 2016, 84: 83. doi: 10.1016/j.measurement.2016.02.005

[12] Ghanbari, K., Fabrication of silver nanoparticles–polypyrrole composite modified electrode for electrocatalytic oxidation of hydrazine, Synth. Met., 2014, 195: 234. doi: 10.1016/j.synthmet.2014.06.014

[13] Saugo, M., Flamini, D.O., Brugnoni, L.I., Saidman, S.B., Silver deposition on polypyrrole films electrosynthesised onto Nitinol alloy. Corrosion protection and antibacterial activity, Mater. Sci. Eng. C Mater. Biol. Appl., 2015, 56: 95. doi: 10.1016/j.msec.2015.06.014PMID: 26249570

[14] Singu, B.S., Yoon, K.R., Synthesis and characterization of MnO_2-decorated graphene for supercapacitors, Electrochim. Acta, 2017, 231: 749. doi: 10.1016/j.electacta.2017.01.182

[15] Singh, A., Salmi, Z., Joshi, N., Jha, P., Decorse, P., Lecoq, H., et al., Electrochemical investigation of free-standing polypyrrole–silver nanocomposite films: a substrate free electrode material for supercapacitors, RSC Adv., 2013, 3: 24567. doi: 10.1039/c3ra42786b

[16] Shimoga, G., Palem, R.R., Choi, D.-S., Shin, E.-J., Ganesh, P.-S., Saratale, G.D., et al., Polypyrrole-based metal nanocomposite electrode materials for high-performance supercapacitors, Metals, 2021, 11: 905. doi: 10.3390/met11060905

[17] González, M.B., Brugnoni, L.I., Vela, M.E., Saidman, S.B., Silver deposition on polypyrrole films electrosynthesized in salicylate solutions,

Electrochim. Acta, 2013, 102: 66. doi: 10.1016/j.electacta.2013.03.116

[18] Deronzier, A., Marques, M.J., Electrodes modified by a Ni-dibenzotetraaza[14]annulene complex via reductive electropolymerization of an α-dibromobenzyl derivative or oxidative electropolymerization of a dipyrrole derivative, J. Electroanal. Chem. Interf. Electrochem., 1989, 265: 341. doi: 10.1016/0022-0728(89)80205-0

[19] Wang, S., Zhang, J., Gharbi, O., Vivier, V., Gao, M., Orazem, M.E., Electrochemical impedance spectroscopy, Nat. Rev. Methods Primers, 2021, 1: 41. doi: 10.1038/s43586-021-00039-w

[20] Hakimi, N., Zouaoui, A., Satour, F.Z., Sahari, A., Zegadi, A., Inorg, J., Electrochemical synthesis and properties of the composite material ITO/polypyrrole-benzoic: Cobalt for electronic storage applications, Organomet. Polym. Mater., 2020, 30: 330. doi: 10.1007/s10904-019-01191-3

[21] Elsherif, O.S., Muftah, G.E.A., Abubaker, O., Dharmadasa, I.M., Structural, optical and electrical properties of SnO_2:F thin films deposited by spray pyrolysis for application in thin film solar cells, J. Mater. Sci. Mater. Electron., 2016, 27: 12280. doi: 10.1007/s10854-016-5206-x

[22] Khaniche, B., Benamrani, H., Zouaoui, A., Zegadi, A., Copper layer elaborated by using different electrochemical methods on ITO/glass substrate, Mater. Sci. Semicond. Proc., 2014, 27: 689. doi: 10.4028/www.scientific.net/amr.1152.65

[23] Vinitha, M., Velraj, G., Synthesis and characteristic studies on pure and nano silver oxide-doped polypyrrole for supercapacitor application, J. Mater. Sci. Mater. Electron., 2022, 33: 6627. doi: 10.1007/s10854-022-07837-2

[24] Lv, J., Liu, Z., Zhang, L., Li, K., Zhang, S., Xu, H., et al., Multifunctional polypyrrole and rose-like silver flower-decorated E-textile with outstanding pressure/strain sensing and energy storage performance, Chem. Eng. J., 2022, 427: 130823. doi: 10.1016/j.cej.2021.130823